Journal of Sensor Science and Technology
Vol. 30, No. 6 (2021) pp. 376-380
http://dx.doi.org/10.46670/JSST.2021.30.6.376
pISSN 1225-5475/eISSN 2093-7563

D-space-controlled graphene oxide hybrid membrane-loaded SnO_2 nanosheets for selective H_2 detection

Ji-Won Jung[1] and Ji-Soo Jang[2,+]

Abstract

The accurate detection of hydrogen gas molecules is considered to be important for industrial safety. However, the selective detection of the gas using semiconductive metal oxides (SMOs)-based sensors is challenging. Here, we describe the fabrication of H_2 sensors in which a nanocellulose/graphene oxide (GO) hybrid membrane is attached to SnO_2 nanosheets (NSs). One-dimensional (1D) nanocellulose fibrils are attached to the surface of GO NSs (GONC membrane) by mixing GO and nanocellulose in a solution. The as-prepared GONC membrane is employed as a sacrificial template for SnO_2 NSs as well as a molecular sieving membrane for selective H_2 filtration. The combination of GONC membrane and SnO_2 NSs showed substantial selectivity to hydrogen gas (R_{air} / R_{gas} > 10 @ 0.8 % H_2, 100 °C) with noise level responses to interfering gases (H_2S, CO, CH_3COCH_3, C_2H_5OH, and NO_2). These remarkable sensing results are attributed mainly to the molecular sieving effect of the GONC membrane. These results can facilitate the development of a highly selective H_2 detector using SMO sensors.

Keywords : Gas sensors, Porous SnO_2, Molecular sieving membranes, Graphene oxide.

1. INTRODUCTION

Hydrogen gas is considered as one of the potential energy sources for various industrial fields because of its abundance in nature and its eco-friendly byproduct (i.e., water) [1]. However, the gas is inherently flammable, colorless, and odorless. Therefore, its leakage should be detected with maximum rapidity [2]. From this perspective, hydrogen gas sensors are required urgently for preventing severe accidents.

The United States Department of Energy (DOE) has set requirements for H_2 sensors, e.g., concentration range (0.1–10%), operating temperature (-30–80 °C), and response time (< 1s) [3]. As a result, substantial efforts have been undertaken to develop highly sensitive and selective H_2 sensors. However, it is challenging to satisfy the above-mentioned requirements.

Among the various types of H_2 sensors, chemiresistive sensors (which are operated by the variations in electrical signals from chemical reactions) have been considered as a potential candidate owing to their rapid response, inexpensive fabrication, and portability. Palladium is conventionally used as a highly effective material for sensing hydrogen gas because of its high selectivity and room-temperature operation [4]. However, Pd-based sensors can be degraded straightforwardly by ambient air and severe volume expansion of Pd. Hence, these sensors are unsuitable for practical use. However, semiconducting metal oxide (SMO)-based chemiresistive sensors have shown high reliability and durability even in ambient air [5]. Nonetheless, SMO-based sensors generally react with numerous gas species, thereby displaying low selectivity toward H_2 gas [6,7].

Here, we propose heterogeneous double-layered H_2 sensors for the first time. These consist of thin-layered SnO_2 nanosheets (NSs) overcoated with a d-space-controlled nanocellulose/graphene oxide (GONC) molecular sieving membrane (SnO_2 NSs@GONC). The d-space of GO was expanded by a nanocellulose fibril buffer layer between GO. This enabled the rapid diffusion of H_2 into the SnO_2 sensing layer. Meanwhile, the GONC molecular sieving layer effectively blocked interfering gas species (e.g., H_2S, CO, acetone, and ethanol). We observed that when a GONC membrane was attached on the SnO_2 sensing layer, GONC selectively filtered hydrogen gas and induced super-selectivity toward it even when the SMO-based sensor was used.

[1] School of Materials Science and Engineering, University of Ulsan (UOU), 14, Techno saneop-ro 55 beon-gil, Nam-gu, Ulsan 44776, Republic of Korea
[2] Center for Electronic Materials, Korea Institute of Science and Technology, 5, Hwarang-ro 14-gil, Seongbuk-gu, Seoul 02792, Republic of Korea
[+]Corresponding author: wkdwltn92@kist.re.kr
(Received: Oct. 12, 2021, Revised: Nov. 19, Nov. 26, 2021, Accepted: Nov. 29, 2021)

2. EXPERIMENTAL

2.1 Synthesis of SnO_2 NSs

Three milliliters of commercialized GO solution (2 mg/mL) was dispersed in 9 mL of ethanol. Then, 0.187 g of an Sn precursor (tin (II) 2-ethylhexanoate) was mixed with ethanol. The as-prepared Sn solution and GO solution were mixed homogeneously. This was followed by magnetic stirring at 250–300 rpm for 12 h [8]. After the stirring process, the Sn precursor-coated GO solution was centrifuged at 3000 rpm for 5 min and subsequently, cleaned two times with ethanol. The collected Sn precursor-coated GO was dried at 60 °C for 12 h. The dried Sn precursor-loaded GO powder was calcined at 400 °C for 1 h (ramping rate: 5 °C/min) to form porous SnO_2 NSs.

2.2 Synthesis of GONC membrane and fabrication of SnO_2 NSs@GONC-sensing device

The commercialized cellulose nanofiber aqueous suspension (0.5 wt%) and GO solution (2 mg/ml) were mixed by the stirring process (w / w = 3 / 7) for 12 h at 300 rpm (GONC solution). To fabricate the sensing device, the porous SnO_2 NSs were dispersed homogeneously in ethanol. Then, the white-colored solution was drop-coated on the interdigitated Au electrode sensor substrate. Subsequently, the as-prepared GONC solution was drop-coated on the SnO_2 sensing layer to form the GONC molecular sieving membrane.

2.3 Gas sensor measurement

The sensing characteristics of each sensor (e.g., SnO_2 NSs, SnO_2 NSs@GO, and SnO_2 NSs@GONC) toward various gas species (e.g., H_2, H_2S, CO, CH_3COCH_3, and C_2H_5OH) were measured at 100 °C. After the sensor stabilization process for 1 h, the target gas species was injected for 10 min at a concentration of 0.1–0.8 %. The sensor was recovered by injecting air for 10 min. Note that all the sensor tests were carried out in a dry condition. The gas responses (R_{air} / R_{gas} to reducing gases) were investigated by a data acquisition system (34972, Agilent). The sensing measurement temperatures were controlled by applying a voltage to the Pt microheater on the backside of the sensor substrate [9].

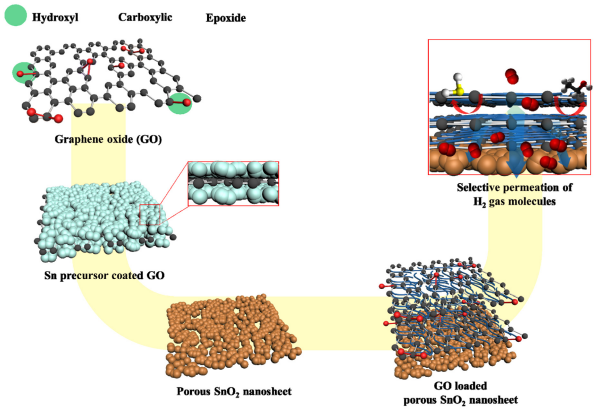

Fig. 1. Schematic illustration of synthesis of SnO_2 NSs@GONC by sacrificial GO templating route and membrane assembly process. Each process is explained in detail in the Experimental Section.

3. RESULTS AND DISCUSSIONS

A key strategy for fabricating SnO_2 nanosheets (NSs) overcoated with a d-space-controlled nanocellulose/graphene oxide (GONC) molecular sieving membrane (hereafter, SnO_2 NSs@GONC) is shown in Fig. 1. First, we employed the GO sacrificial templating route for synthesizing porous SnO_2 NSs as a chemiresistive sensing layer [10]. Owing to the strong chemical interaction between numerous functional groups on the GO NSs and Sn precursors, the Sn precursor molecules were decorated uniformly on the GO surface (Fig. 1) [11]. Then, the Sn precursor-loaded GO NSs were calcined at 400 °C for 1 h to form porous SnO_2 NSs.

Owing to the thermal decomposition of GO and oxidation of the Sn precursor, the porous SnO_2 NSs were formed after the calcination process. The nanocellulose and GO NSs were employed as a gas filtering membrane. Note that the nanocellulose was used for a d-spacing controller of GO NSs. By applying the simple solution mixing process with nanocellulose and GO NS aqueous solution, nanocellulose fibers were induced to self-assemble on the GO NSs (GONC). Then, the as-prepared SnO_2 NSs were drop-coated on the sensing substrate, and a GONC membrane was decorated on the SnO_2 NSs using the solution drop-coating method. Nanocellulose can play a critical role as a filler layer between GO NSs and thereby, expand the d-space channel pores of GO NSs. As a result, target hydrogen gas molecules may diffuse rapidly into GONC through expanded channel pores of GONC, and interfering gas analytes can be

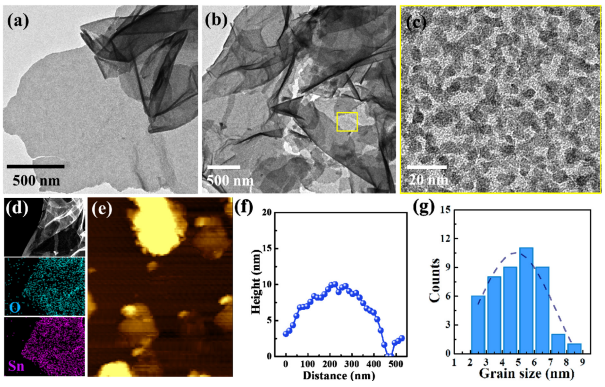

Fig. 2. TEM images of (a) Sn precursor-assembled GO (Sn-GO NSs), (b, c) porous SnO_2 NSs after heat treatment at 400 °C, (d) energy dispersive spectroscopy (EDS) mapping of SnO_2 NSs, (e, f) atomic force microscopy (AFM) analysis of SnO_2 NSs and thickness distribution, (g) grain size distribution of SnO_2 NSs.

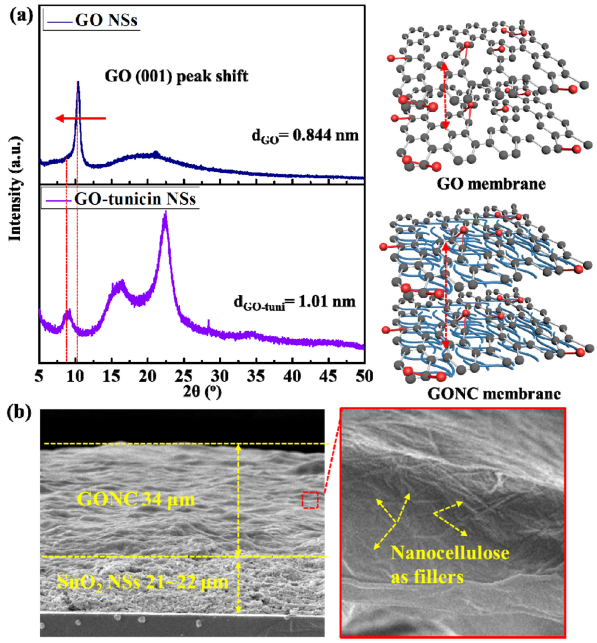

Fig. 3. (a) X-ray diffraction (XRD) patterns of GO and GONC with corresponding d-space values, and schematic images of GO and GONC, (b) cross-sectional SEM images of SnO_2 NSs@GONC, and magnified image of GONC surface.

blocked effectively by the surface pores of GONC.

The microstructures of the porous SnO_2 NSs were investigated by a transmission electron microscope (TEM). As shown in Fig. 2(a), Sn precursors were decorated uniformly on the GO NSs (hereafter, Sn-GO NSs), thereby exhibiting ultrathin two-dimensional (2D) morphology. After the calcination step, the TEM image of SnO_2 NSs exhibited morphological characteristics similar to those of Sn-GO NSs. This implies that the GO NSs effectively function as a sacrificial template for 2D morphological SnO_2 NSs during the calcination process (Fig. 2(b)). Furthermore, the sub-10 nm grain sizes of SnO_2 induce a high porosity. This is shown in the magnified TEM image of SnO_2 NSs (Fig. 2(c)). Moreover, energy dispersive spectroscopy (EDS) mapping analysis verified that Sn and O were distributed homogeneously on the SnO_2 NSs (Fig. 2(d)). Atomic force microscope (AFM) analysis was carried out to further investigate the thickness of the SnO_2 NSs (Fig. 2(e)). The AFM result clearly reveals that the SnO_2 NSs exhibited sub-10 nm thickness with a grain size distribution of 4–6 nm (Fig. 2(f), (g)).

To investigate the channel pores of the d-space-controlled GONC membrane, we carried out high-resolution X-ray diffraction (XRD) analysis with GO and GONC samples. We can accurately estimate the d-space values of GO and GONC using Bragg's law on XRD peaks of GO and GONC samples, respectively. As shown in Fig. 3(a), GONC showed a large d-space value (1.01 nm) compared with GO (0.844 nm). This implies that one-dimensional (1D) nanocellulose between GO NSs plays an effective role as a filler layer for increasing the d-space of GO NSs (schematic image in Fig. 3(a). Based on the cross-sectional scanning electron microscope (SEM) result, we verified that the 34 μm-thick GONC membrane was decorated uniformly on the 21–22 μm-thick SnO_2 NSs (Fig. 3(b)). Furthermore, nanocellulose as a filler between GO membranes was observed by magnified SEM analysis (red box image in Fig. 3(b)).

The sensing measurement test was carried out using the three samples (i.e., SnO_2 NSs, SnO_2 NSs@GO, and SnO_2 NSs@GONC) to investigate the membrane effect on gas sensing characteristics. Note that we conducted sensing tests with various gas species including H_2, H_2S, CO, CH_3COCH_3, and C_2H_5OH. To fabricate the sensing devices, the porous SnO_2 NSs were drop-coated on an aluminum sensing substrate having an interdigitated Au electrode (width = 25 μm; gap size = 150 μm) [12]. Then, the GO or GONC molecular sieving membrane was overcoated on the SnO_2 NSs sensing layer. As shown in Fig. 4(a), pristine SnO_2 NSs and SnO_2 NSs@GONC sensors showed significant H_2 responses (R_{air} / R_{gas} > 10 @ 0.8 % H_2), whereas SnO_2 NSs@GO exhibited relatively low H_2 responses (R_{air} / R_{gas} < 5 @ 0.8 % H_2). Moreover, SnO_2 NSs@GO showed low H_2 responses over a wide range of hydrogen-gas concentration compared with SnO_2 NSs and SnO_2 NSs@GONC (Fig. 4(b)). These sensing behaviors indicate that the pristine GO membrane having a small d-space (0.844 nm) could disrupt the gas diffusion into the SnO_2 sensing

layer. Meanwhile, the GONC membrane showed high H_2 permeability considering the H_2 response of SnO_2 NSs@GONC. Because the d-space pores of GONC were expanded by the nanocellulose filler layer, the GONC membrane could show significantly higher H_2 permeability. To investigate the selectivity properties of each sensor, we compared the gas responses to H_2S, CO, CH_3COCH_3, and C_2H_5OH. The comparison results revealed that SnO_2 NSs showed low selective sensing properties owing to the high responses to various gases (R_{air} / R_{gas} > 5 for H_2S, CH_3COCH_3, and C_2H_5OH) (Fig. 4(c)). However, it is noteworthy that SnO_2 NSs@GO and SnO_2 NSs@GONC showed negligible responses to H_2S, CH_3COCH_3, CO, and C_2H_5OH (Fig. 4(c)). This implies that GO and GONC membranes effectively blocked the interfering gas species (H_2S, CO, CH_3COCH_3, C_2H_5OH) owing to their large kinetic diameter (0.360 nm, 0.376 nm, 0.460 nm, and 0.450 nm, respectively). In general, the surface pores of the GO-based membrane had sub-0.3 nm sizes and thereby, blocked the larger gas molecules [13]. However, H_2 molecules having a kinetic diameter of 0.289 nm could pass through the GO surface, and the expanded d-space of GONC could accelerate the diffusion of H_2 molecules to the SnO_2 sensing layer.

Based on these principles, the SnO_2 NSs@GONC sensor showed a higher H_2 selectivity than the SnO_2 NSs and SnO_2 NSs@GO sensors (Fig. 4(d)). Note that we used S_{H2} / S_{H2S} as an H_2 selectivity factor because the response of the SnO_2 NS-based sensor to H_2S was the dominant response to interfering analytes.

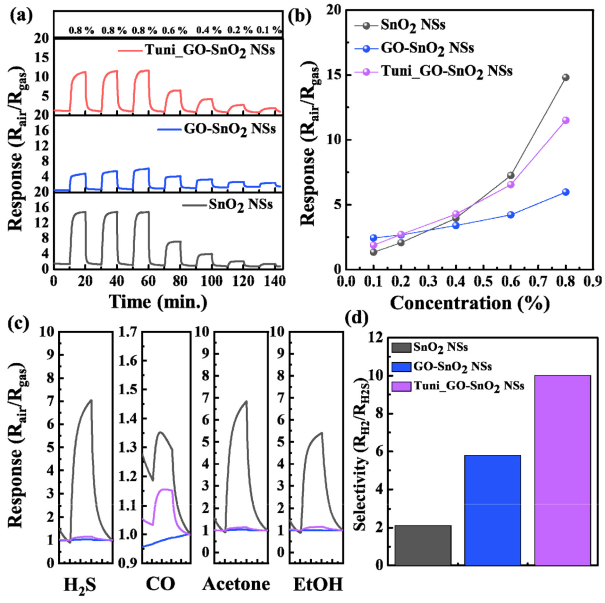

Fig. 4. (a) Hydrogen gas sensing properties of SnO_2 NS-, SnO_2 NSs@GO-, and SnO_2 NSs@GONC-based sensors, (b) graph of hydrogen gas response values with respect to hydrogen gas concentration, for each sensor, (c) sensing response kinetics of each sensor to H_2S, CO, acetone, and ethanol, (d) sensing selectivity plots of SnO_2 NS-, SnO_2 NSs@GO-, and SnO_2 NSs@GONC-based sensors

5. CONCLUSIONS

To summarize, we successfully developed the d-space-controlled (0.844–1.01 nm) GONC membrane for exceptional H_2 sensing selectivity. Because of the self-assembly of nanocellulose on the GO NSs, the GONC membrane had expanded d-space pores compared with the conventional GO membrane. Furthermore, we combined the GONC membrane with the SnO_2 NSs-based sensing layer by a simple drop-casting method. Because of the synergistic effect between the GONC membrane (molecular sieving layer) and porous SnO_2 NSs (sensing layer), the SnO_2 NSs@GONC sensor showed a dramatically enhanced selectivity to hydrogen gas. The miniscule size of the surface pores of GONC can effectively block the interfering gas species, whereas the expanded d-space of GONC enables the acceleration of H_2 diffusion to the SnO_2 sensing layer. Based on this improvement, d-space-controlled GO-based membrane combined with sensing layer would facilitate the control of the gas selectivity of chemiresistive gas sensors.

ACKNOWLEDGMENTS

This work was supported by a National Research Foundation of Korea (NRF) grant funded by the Korean government (MSIT) (No. 2021R1F1A1060285).

REFERENCES

[1] J. S. Jang, S. Qiao, S.-J. Choi, G. Jha, A. F. Ogata, W. T. Koo, D. H. Kim, I. D. Kim, R. M. Penner, “Hollow Pd–Ag composite nanowires for fast responding and transparent hydrogen sensors”, *ACS Appl. Mater. Interfaces*, Vol. 9, No. 45, pp. 39464-39474, 2017.

[2] W. T. Koo, S. Qiao, A. F. Ogata, G. Jha, J. S. Jang, V. T. Chen, I. D. Kim, and R. M. Penner, “Accelerating palladium nanowire H2 sensors using engineered nanofiltration”, *ACS Nano*, Vol. 11, No.9, pp. 9276-9285, 2017.

[3] W. T. Koo, H. J. Cho, D. H. Kim, Y. H. Kim, H. Shin, R. M. Penner, and I. D. Kim, “Chemiresistive hydrogen sensors: fundamentals, recent advances, and challenges”, *ACS Nano*, Vol. 14, No.11, pp. 14284-14322, 2020.

[4] S. Y. Cho, H. Ahn, K. Park, J. Choi, H. Kang, and H. T.

Jung, “Ultrasmall grained Pd nanopattern H2 sensor”, *ACS Sens.*, Vol. 3, No.9, pp. 1876-1883, 2018.

[5] S. J. Kim, S. J. Choi, J. S. Jang, H. J. Cho, and I. D. Kim, “Innovative nanosensor for disease diagnosis”, *Acc. Chem. Res.,* Vol. 50, No. 7, pp. 1587-1596, 2017.

[6] J. S. Jang, J. Lee, W. T. Koo, D. H. Kim, H. J. Cho, H. Shin, and I. D. Kim, “Pore-size-tuned graphene oxide membrane as a selective molecular sieving layer: toward ultraselective chemiresistors”, *Anal. Chem.,* Vol. 92, No. 1, pp. 957-965, 2019.

[7] J. S. Jang, W. T. Koo, S. J. Choi, and I. D. Kim, “Metal organic framework-templated chemiresistor: sensing type transition from p-to-n using hollow metal oxide polyhedron via galvanic replacement”, *J. Am. Chem. Soc.,* Vol. 139, No. 34, pp. 11868-11876, 2017.

[8] J. S. Jang, S. Cho, H. J. Han, S. W. Song, S. J. Kim, W. T. Koo, D. H. Kim, H. Jeong, Y. S. Jung, and I. D. Kim, “Universal Synthesis of Porous Inorganic Nanosheets via Graphene-Cellulose Templating Route”, *ACS Appl. Mater. Interfaces,* Vol. 11, No.37, pp. 34100-34108, 2019.

[9] J. S. Jang, S. J. Choi, S. J. Kim, M. Hakim, and I. D. Kim, “Rational design of highly porous SnO2 nanotubes functionalized with biomimetic nanocatalysts for direct observation of simulated diabetes”, *Adv. Funct. Mater.,* Vol. 26, No. 26, pp. 4740-4748, 2016.

[10] J. S. Jang, Y. W. Lim, D. H. Kim, D. Lee, W. T. Koo, H. Lee, B. S. Bae, and I. D. Kim, “Glass?Fabric Reinforced Ag Nanowire/Siloxane Composite Heater Substrate: Sub?10 nm Metal@ Metal Oxide Nanosheet for Sensitive Flexible Sensing Platform”, *Small,* Vol. 14, No. 44, pp. 1802260(1)-1802260(10), 2018.

[11] R. Kim, J. S. Jang, D. H. Kim, J. Y. Kang, H. J. Cho, Y. J. Jeong, and I. D. Kim, “A general synthesis of crumpled metal oxide nanosheets as superior chemiresistive sensing layers”, *Adv. Funct. Mater.,* Vol. 29, No.31, pp. 1903128(1)-1903128(10), 2019.

[12] J. S. Jang, J. K. Kim, K. Kim, W. G. Jung, C. Lim, S. Kim, D. H. Kim, B. J. Kim, J. W. Han, W. Jung, and I. D. Kim, “Dopant-Driven Positive Reinforcement in Ex?Solution Process: New Strategy to Develop Highly Capable and Durable Catalytic Materials”, *Adv. Mater.,* Vol. 32, No. 46, pp. 2003983(1)-2003983(9), 2020.

[13] J. S. Jang, H. J. Jung, S. Chong, D. H. Kim, J. Kim, S. O. Kim, and I. D. Kim, “2D materials decorated with ultrathin and porous graphene oxide for high stability and selective surface activity”, *Adv. Mater.,* Vol. 32, No. 36, pp. 2002723(1)-2002723(10), 2020.